

Effects of Magnetic and non-Magnetic Impurities on the Superconducting State of $\text{YBa}_2\text{Cu}_3\text{O}_{7-\delta}$

M. Le Tacon,^{1,2} A. Sacuto,^{1,2} Y. Gallais,³ E. Ya. Sherman,⁴ A. Forget,⁵ and D. Colson⁵

¹*Laboratoire Matériaux et phénomènes Quantiques (UMR 7162 CNRS),
Université Paris 7, 2 place Jussieu 75251 Paris, France*

²*Laboratoire de Physique du Solide ESPCI, 10 rue Vauquelin 75231 Paris, France*

³*Departments of Physics and Applied Physics, Columbia University New York, NY 10027, USA*

⁴*Department of Physics and Institute for Optical Sciences,*

University of Toronto, 60 St. George St., Toronto M5S 1A7, Ontario, Canada

⁵*Service de Physique de l'Etat Condensée, CEA-Saclay, 91191 Gif-sur-Yvette, France*

(Dated: December 15, 2018)

We report electronic Raman scattering measurements on initially optimally doped Zn and Ni substituted Y-123 in A_{1g} and B_{1g} channels. We show that the B_{1g} superconducting gap is independent of magnetic Ni and non-magnetic Zn impurity concentrations. On the contrary, the energy of the A_{1g} collective mode follows T_c with two distinct slopes for Ni and Zn impurities, tracking the magnetic resonance detected by neutrons. We explain the unconventional behavior of the B_{1g} superconducting gap and discuss the evolution of the A_{1g} mode under Ni and Zn impurities.

PACS numbers: 74.62.Dh, 74.72.-h, 78.30.-j

In the last few years, transport [1], nuclear magnetic resonance (NMR) [2], muon spin relaxation (μ -SR) [3, 4] and scanning tunneling microscopy (STM) [5] measurements have shown that the effects of magnetic and non-magnetic impurities on the superconducting properties of cuprates are drastically different. Therefore they can be used as relevant probes for testing the quasiparticles and the collective modes in the superconducting state of cuprates. Electronic Raman scattering (ERS) is a powerful tool for probing electronic excitations in selected areas of the Fermi surface. Raman responses are very sensitive to the d -wave character of the superconducting gap (SG). The B_{1g} channel [6] probes the antinodal regions where the SG amplitude 2Δ is maximum while the B_{2g} channel [6] probes the nodal regions where the SG vanishes. The A_{1g} channel [6] has no symmetry restriction and is sensitive to nodal and antinodal regions of the Fermi surface. In the A_{1g} channel an intense Raman active collective mode (the " A_{1g} mode"), which origin is not yet identified, is definitively observed in the superconducting state of optimally doped cuprates [7], well below the 2Δ energy. It has been shown that the A_{1g} mode tracks the magnetic resonance detected by inelastic neutron scattering [8] at $\mathbf{Q}_{AF} = (\pi, \pi)$ for both its temperature and energy dependence under magnetic Ni substitutions. Previous ERS studies on Zn substituted Y-123 with only one Zn concentration lead to contradictory results: on one hand the 2Δ energy of the SG seen in the B_{1g} channel follows T_c [9], on the other hand it was argued to collapse to zero [10] when $T_c = 72$ K. Here we report ERS measurements on a wide concentration range of Zn impurities and compare them with those of Ni magnetic impurities. We show unambiguously that the 2Δ energy of the SG in B_{1g} channel remains constant under magnetic and non-magnetic impurity substitutions

up to 3%, in contradiction with what we expect from a conventional superconductor. We show that the energy of the A_{1g} mode follows T_c with two distinct slopes for Zn and Ni impurities and tracks the magnetic resonance energy does. Using an intermediate scattering potential with anisotropic phase shift for Ni impurities and an unitary limit scattering in the "Swiss Cheese" [3] model for Zn impurities, we explain the unexpected B_{1g} SG energy dependence and discuss the A_{1g} collective mode behavior.

Studied samples were optimally doped $\text{YBa}_2(\text{Cu}_{1-y_{\text{Zn}}}\text{Zn}_{y_{\text{Zn}}})_3\text{O}_{7-\delta}$ single crystals (grown by the "self-flux" method [11]) with various Zn concentrations: $y_{\text{Zn}}=0$ ($T_c^{\text{(onset)}}=92.5\text{K}$; $\Delta T_c \sim 2$ K), $y_{\text{Zn}}=0.3\%$ (87.5K; 2K), $y_{\text{Zn}}=0.7\%$ (83K; 3K), $y_{\text{Zn}}=1.5\%$ (73K; 4K) and $y_{\text{Zn}}=2\%$ (64K; 7K). They have been renamed Y-123, Y-123:Zn87K, Y-123:Zn83K, Y-123:Zn73K and Y-123:Zn64K respectively. Similarly, the Ni substituted Y-123 crystals of [8], have been renamed Y-123:Ni87K and Y-123:Ni78K. Impurity concentrations were checked by chemical analysis using an electron probe. $T_c^{\text{(onset)}}$ and 10%-90% width ΔT_c have been evaluated from ZFC DC-magnetization under a 10G field. The broadening of transition under impurity substitutions is consistent with previous works (see e.g. Ref. [12] and references therein). Zn and Ni are divalent ions known to offer a particularly attractive way to reduce T_c without changing the carrier concentrations [13].

ERS have been carried out with a T64000 JY spectrometer in triple subtractive configuration. Crystals were mounted on the cold finger of an He circulation cryostat and cooled down to 10 K. The 514nm excitation line was used. The laser power on the crystal surface was kept below 3mW to avoid significant heating (which is smaller than 3K according to Stokes-anti-Stokes ra-

tio). Raw spectra have been corrected for the Bose factor $n(\Omega, T)$ to get the imaginary part of the Raman susceptibility $\chi''(\Omega) = I(\Omega)/[1 + n(\Omega, T)]$.

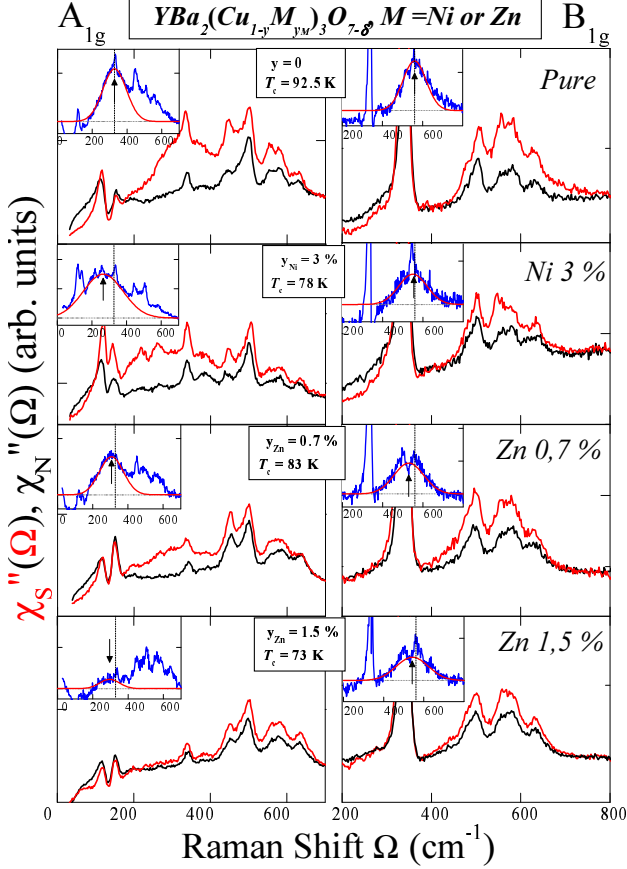


FIG. 1: Superconducting and normal Raman responses $\chi''_S(\Omega)$ (in red) and $\chi''_N(\Omega)$ (in black) of selected $\text{YBa}_2(\text{Cu}_{1-y_M}\text{M}_{y_M})_3\text{O}_{7-\delta}$ ($\text{M} = \text{Ni}, \text{Zn}$) single crystals. The difference $\chi''_S(\Omega) - \chi''_N(\Omega)$ (in blue) is plotted in the insets.

Figure 1 shows the susceptibilities $\chi''_N(\Omega)$ (resp. $\chi''_S(\Omega)$) in normal (resp. superconducting) state in the A_{1g} and B_{1g} channels for selected concentrations ($y_{\text{Ni}}=3\%$, $y_{\text{Zn}}=0.7\%$ and 1.5%) of Ni and Zn impurities. The spectra related to $y_{\text{Ni}}=1\%$, $y_{\text{Zn}}=0.3\%$ and 2% are not shown here and can be found in Refs. [7, 8]. The phonon lines for both A_{1g} and B_{1g} channel are well identified as well as additional weak features related to slight CuO chains disorder [8]. For pure Y-123, we have a clear enhancement of the A_{1g} and B_{1g} electronic responses between $(170\text{--}670\text{ cm}^{-1})$ and $(400\text{--}800\text{ cm}^{-1})$ respectively in the superconducting state compared to the normal one. Subtractions of the normal contribution from the superconducting one are shown in insets. In B_{1g} channel, we obtain a well defined peak centered at 565 cm^{-1} ($8.8 k_B T_c$) corresponding to the 2Δ pair breaking energy of the SG. In the A_{1g} channel, the subtraction gives rise to a broad asymmetric peak, in which two distinct contributions have already been established [7]. The first one is the A_{1g} collective mode centered at 331 cm^{-1} ($5 k_B T_c$),

that runs from 170 to 410 cm^{-1} and the second one, from 410 to 670 cm^{-1} is the SG signature in the A_{1g} channel [7].

As Ni impurities are introduced the A_{1g} mode softens and broadens but does not exhibit any significant decrease of its intensity up to $y_{\text{Ni}}=3\%$. On the contrary the A_{1g} mode under Zn impurities reduces to a weak contribution around 295 cm^{-1} for $y_{\text{Zn}}=1.5\%$ and totally disappears for $y_{\text{Zn}}=2\%$ [7]. On the other hand, the B_{1g} SG broadens but remains almost constant in energy with respect to Ni and Zn impurity insertions, in contrast with the A_{1g} mode which shifts to lower energy.

In Fig. 2 are reported the A_{1g} mode and the B_{1g} SG energies with respect to T_c for all Ni and Zn impurity concentrations. In addition to our measurements we have plotted the data of Ref.[10]. In contrast to what we expect from a conventional superconductor, the 2Δ SG energy remains almost constant as T_c decreases with Ni and Zn impurities. In particular our experimental data show that the B_{1g} SG energy in Y-123:Zn neither falls to zero as T_c reaches 72 K (as claimed in Ref. [10]), nor scales with T_c (see Ref. [9]) but remains constant in energy over a wide concentration range down to $T_c = 64\text{ K}$. Its average value (2Δ) is $\sim 67.6\text{ meV}$ ($\pm 2.5\text{ meV}$). It has already been shown that changes of T_c under oxygen doping fail to keep the $2\Delta/k_B T_c$ ratio constant, and our data show that even for fixed doping (here the optimal one), when T_c decreases under magnetic or non-magnetic impurities substitutions, $2\Delta/k_B T_c$ is not constant anymore.

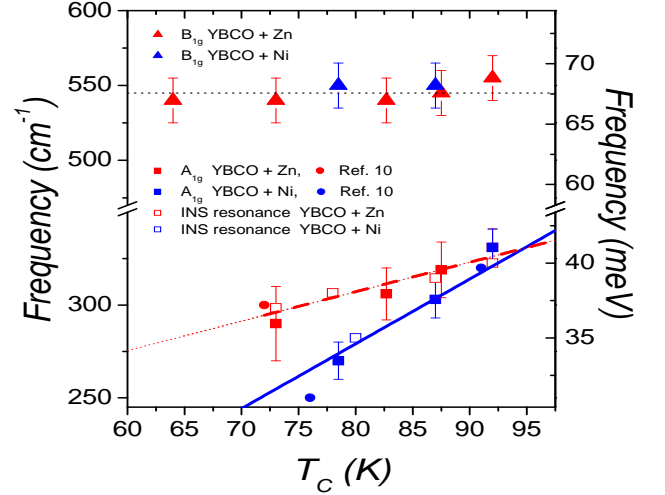


FIG. 2: Energies of the SG peak (triangles), A_{1g} mode (filled squares) and of the neutron resonance (empty squares) with respect to T_c under magnetic Ni (blue) and non magnetic Zn (red) impurity substitutions. Data from reference 10 have been added as filled circles.

Figure 2 shows that the A_{1g} mode energy softens faster for Ni impurities than for the Zn one: the energy of A_{1g} mode follows $5k_B T_c$ for Ni, whereas it follows, for Zn, $k_B(2.2T_c + 2.8T_c^{\text{opt}})$, where $T_c^{\text{opt}} = 92.5\text{ K}$ is the optimal T_c of Y-123. We notice that the data of Ref.[10] follows the two distinct A_{1g} slopes for Ni and Zn impurities.

This confirms that the " A_{1g} -mode-energy/ T_c " ratio is not constant (and not equal to $5k_B$) for Zn substitutions.

From STM measurements it has been shown that the quasiparticle scattering on Ni impurities is predominantly potential, rather than magnetic [14]. Based on this finding, we have calculated the superconducting density of states (SDOS) and the B_{1g} Raman response for a CuO_2 plane where Cu is substituted by Ni. Considering potential pair breaking in a d -wave model, described by the usual Nambu-Gorkov' Green functions (see e.g., Ref.[17]) The SDOS and the imaginary part of the B_{1g} Raman response are given by:

$$N_S(\Omega) = -\frac{1}{\pi} \Im \sum_{\mathbf{k}} \text{Tr} \hat{G}(\mathbf{k}, i\omega_n) \big|_{i\omega_n \rightarrow \Omega + i0^+}, \quad (1)$$

and

$$\chi''_{B_{1g}}(\Omega) = -T \Im \sum_{\mathbf{k}} \sum_{\omega_n} \gamma_{B_{1g}}(\mathbf{k})^2 \text{Tr} [\hat{\tau}_3 \hat{G}(\mathbf{k}, i\omega_n) \times \hat{\tau}_3 \hat{G}(\mathbf{k}, i\omega_n - i\Omega_m)] \big|_{i\Omega_m \rightarrow \Omega + i0^+}, \quad (2)$$

where $\gamma_{B_{1g}}(\mathbf{k})$ is the B_{1g} Raman vertex calculated in the effective mass approximation, and ω_n and Ω_m are fermionic and bosonic Matsubara frequencies, respectively. The details of calculation will be published elsewhere. Scattering in the Born ($\delta = 0$) and unitary ($\delta = \pi/2$) limits have already been treated in previous works [15, 16]. As scattering on Ni impurities is between these two limits [14], we have opted for an intermediate momentum dependent phase shift $\delta(\mathbf{k})$, due to the anisotropy of the Fermi velocity v_F . The self energy $\Sigma(i\omega_n)$ is then given by [17]:

$$\Sigma(i\omega_n) = \frac{n_{\text{imp}} \sum_{\mathbf{k}} \tan(\delta(\mathbf{k}))^2 \text{Tr} \hat{G}(\mathbf{k}, i\omega_n)}{(\pi N_F)^2 - [\sum_{\mathbf{k}} \tan(\delta(\mathbf{k})) \text{Tr} \hat{G}(\mathbf{k}, i\omega_n)]^2} \quad (3)$$

where n_{imp} stands for Ni impurity concentration, and N_F for the DOS at the Fermi level in the normal state.

In Fig. 3, we have plotted the B_{1g} Raman response as a function of Raman shift Ω for different n_{imp} (up to 5%). The SDOS $N_S(\Omega)$ is plotted in inset. At $\Omega = 2\Delta_0$ (resp. $\Omega = \Delta_0$), with no impurities, $\chi''_{B_{1g}}$ (resp. $N_S(\Omega)$) diverges logarithmically. As Ni impurities are inserted, both $\chi''_{B_{1g}}$ and N_S exhibit a maximum at the same energy than in the pristine case, suggesting that the quasiparticles in the antinodal regions are not affected by impurity scattering. The intensity of $\chi''_{B_{1g}}(2\Delta_0)$ decreases with increasing n_{imp} , just as observed experimentally. A finite DOS appears at the Fermi level $\Omega = 0$, and increases with n_{imp} . Low energy excitations in the superconducting state come from quasiparticles of the nodal regions. $N_S(\Omega = 0)$ grows when n_{imp} increases implies that superconductivity is destroyed around the nodes of the SG, where the interaction leading to the Cooper pairs formation is weaker. This is consistent with B_{2g} Raman

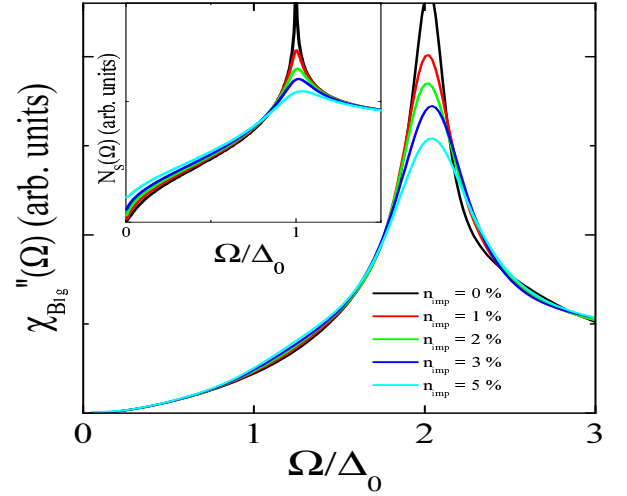


FIG. 3: Evolution of the B_{1g} Raman response as a function of impurity concentration for a d -wave superconductor. Δ_0 is the energy of the SG in the pristine case. The SDOS is plotted in inset.

data [18] which reveals no distinctions between superconducting and normal B_{2g} responses as from 1% of Ni impurities. This explains also why the B_{2g} response is more generally affected by any scattering source (e.g. structural disorder) as previously observed [18, 19, 20]. The situation is different for non-magnetic impurities since the scattering has been found to be almost unitary ($\delta \sim 0.48\pi$ [5]). As a consequence, the superconducting order parameter is suppressed locally around each impurity site, and the superfluid density decreases. This gives rise to the "Swiss Cheese" model and explains why the SG intensity decreases as Zn concentration increases. To achieve the calculation of DOS and Raman response in a Zn substituted cuprate, a serious difficulty arises from the fact that one must take into account spatial inhomogeneities of the superconducting order parameter. It has not been performed here. However, our data suggest that, in the remaining superconducting condensate, the Cooper pairs binding energy is not altered, and thus no changes are seen in the pair breaking peak in the B_{1g} channel.

At this step, it is interesting to notice that non-magnetic impurity effects in cuprates, at least on transport and T_c , can be reproduced by defects induced by electron irradiation [1]. Angle resolved photoemission spectroscopy (ARPES) measurements performed on such irradiated samples (Bi-2212 with a T_c down to 62 K) have revealed no changes in the SG energy with respect to T_c [21]. This is consistent with our data. In Fig. 2, we have added to the A_{1g} mode energies under Ni and Zn substitutions, the magnetic resonance energies obtained from [22]. This shows unambiguously that for these two substitutions, the A_{1g} mode tracks the magnetic resonance. As a consequence, magnetic and non-magnetic impurities lead to two different slopes for both the A_{1g} mode and the magnetic resonance.

To go further, we have plotted in Fig. 4 the temperature dependences of the A_{1g} mode for four crystals Y-123, Y-123:Zn83K, Y-123:Ni87K and Y-123:Ni78K.

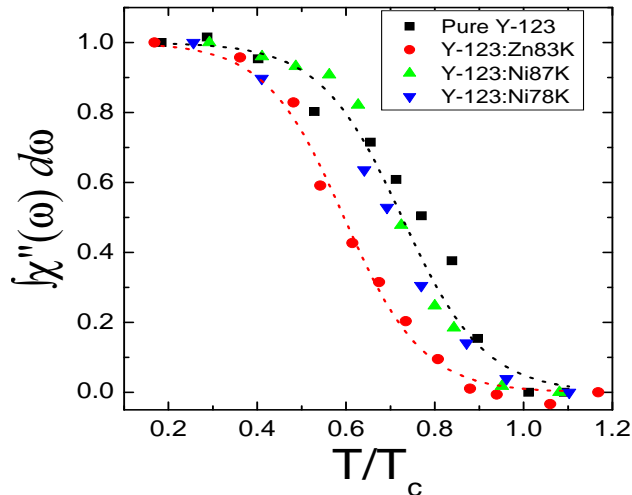


FIG. 4: Temperature dependences of the spectral weight between 170 cm^{-1} and 420 cm^{-1} of the A_{1g} mode. The temperature scale has been normalized to T_c for each crystal.

We clearly see that the A_{1g} mode starts growing just below T_c in Y-123:Ni, in the same way as pure Y-123. On the contrary, in the Zn case the A_{1g} mode exhibits a relative temperature delay of $0.8 k_B T_c$ ($\sim 20\text{ K}$). This has also been observed in Ref. [10]. For Ni impurities, the A_{1g} mode spectral weight follows the one of the free Y-123 as function of temperature. The energies of both A_{1g} mode and magnetic resonance follow $5 k_B T_c$ for Ni-substituted and pure Y-123 (Fig. 2), and STM measurements have shown the presence of localized states on the Ni impurity, but no disruption of superconductivity near the impurity [14]. These three experimental observations suggest that superconductivity is homogeneously modified by the introduction of magnetic impurities, and that the mechanism that leading to the formation of both magnetic resonance and A_{1g} mode is not fundamentally affected, but rather renormalized with respect to T_c . The scenario is different for Zn impurities. On one hand, the shift in energy for both the A_{1g} mode and magnetic resonance is smaller than for Ni impurities (Fig. 2). On the other hand, (see Fig. 1) the intensity of the A_{1g} mode decreases strongly with increasing Zn concentration, and for a concentration greater than 2% this mode disappears, in contrast with Ni substitutions [8]. Finally, Fig. 4 shows that the A_{1g} mode starts growing 20 K below T_c in the Y-123:Zn83K crystal. Consequently, there exist Zn concentrations where superconductivity has settled, but the A_{1g} mode is already not present. This brings us to the conclusion that the diminution of superfluid density observed in μ -SR [3, 4] for Zn-substituted samples does not explain alone the disappearance of the A_{1g} mode. As it has been shown previously, AF fluctuations at $\mathbf{Q}_{AF} = (\pi, \pi)$ are strongly enhanced above T_c in Zn-substituted samples [22], and survive in the su-

perconducting state. We believe that these fluctuations put back the A_{1g} mode and the neutron resonance [22], and that the disappearance of these two collective modes when Zn concentration is larger than 2% results from a conjugate effect of AF fluctuations and the diminution of the superfluid density.

In conclusion, we have shown that the unconventional behavior of the B_{1g} SG can be explained under anisotropic potential scattering for Ni magnetic substitutions. Through Zn non-magnetic substitutions, we have confirmed the strong link between the magnetic resonance and the A_{1g} mode. The A_{1g} mode in Zn substituted Y-123 exhibits a significant temperature delay from T_c in comparison to the one in the Ni substituted Y-123 due to the presence of strong antiferromagnetic fluctuations.

Acknowledgments: We thank S. Pailhès, Y. Sidis, Ph. Bourges, M. Cazayous, K. Behnia, G. Deutscher, and P. Monod for very fruitful discussions.

-
- [1] F. Rullier-Albenque, P.A. Viennefond, H. Alloul, A.W. Tyler, P. Lejay, and J.F. Marucco, Phys. Rev. Lett. **91**, 047001 (2003).
 - [2] J. Bobroff, W.A. MacFarlane, H. Alloul, P. Mendels, N. Blanchard, G. Collin, and J.F. Marucco, Phys. Rev. Lett. **83**, 4381 (1999).
 - [3] B. Nachumi, A. Keren, K. Kojima, M. Larkin, G.M. Luke, J. Merrin, O. Tchernyshov, Y.J. Uemura, N. Ichikawa, M. Goto, and S. Uchida, Phys. Rev. Lett. **77**, 5421 (1996).
 - [4] C. Bernhard, J.L. Tallon, C. Bucci, R. De Renzi, G. Guidi, G.V.M. Williams, and Ch. Niedermayer, Phys. Rev. Lett. **77**, 2304 (1996).
 - [5] S.H. Pan, E. W. Hudson, K. M. Lang, H. Eisaki, S. Uchida, and J. C. Davis, Nature **403**, 746 (2000).
 - [6] B_{2g} and B_{1g} channels are obtained from cross polarizations of the incident and scattered electric fields along and at 45° from the Cu-O bounds of CuO_2 layers. Parallel polarizations at 45° from the Cu-O bounds give the $A_{1g}+B_{2g}$ channel, and pure A_{1g} channel is obtained by subtracting the B_{2g} one from the $A_{1g}+B_{2g}$ one.
 - [7] M. Le Tacon, A. Sacuto, and D. Colson, Phys. Rev. B **71**, R100504 (2005).
 - [8] Y. Gallais, A. Sacuto, P. Bourges, Y. Sidis, A. Forget, and D. Colson, Phys. Rev. Lett. **88**, 177401 (2002).
 - [9] M. Limonov, D. Shantsev, S. Tajima, and A. Yamanaka, Phys. Rev. B **65**, 024515 (2001).
 - [10] H. Martinho, A.A. Martin, C. Rettori, and C. T. Lin, Phys. Rev. B **69**, 180501 (2004).
 - [11] D. L. Kaiser, F. Holtzberg, B. A. Scott, and T.R. McGuire, Appl. Phys. Lett. **51**, 1040 (1987).
 - [12] H. F. Fong, P. Bourges, Y. Sidis, L. P. Regnault, J. Bossy, A. Ivanov, D. L. Milius, I. A. Aksay, and B. Keimer Phys. Rev. Letters **78**, 1939(1999)
 - [13] A.V. Mahajan, H. Alloul, G. Collin, and J.F. Marucco, Phys. Rev. Lett. **72**, 3100 (1994); J. Bobroff, H. Alloul, P. Mendels, V. Viallet, J.F. Marucco, and D. Colson, Phys. Rev. Lett. **78**, 3757 (1997).

- [14] E. W. Hudson, K. M. Lang, V. Madhavan, S. H. Pan, H. Eisaki, S. Uchida, and J. C. Davis, *Nature* **411**, 920 (2001).
- [15] R. Fehrenbacher and M.R. Norman *Phys. Rev. B* **50**, R3495 (1994); L.S. Borkowski and P.J. Hirschfeld, *Phys. Rev. B* **49**, R15404 (1994).
- [16] T.P. Devereaux, *Phys. Rev. Lett.* **74**, 4313 (1995).
- [17] V.P. Mineev and K.V. Samokhin, *Introduction to Unconventional Superconductivity*, Gordon and Breach, Amsterdam (1999); J.-M. Tang and M. E. Flatté, *Phys. Rev. B* **66**, R060504 (2002).
- [18] Y. Gallais, Thèse de Doctorat de l'Université Paris VI (2003), available at <http://ufrphy.lbhp.jussieu.fr/mpq/recherche/electronique/conduteurs/conduteursGallaisColsonGautierPicard.pdf>
- [19] Y. Gallais, A. Sacuto, T.P. Devereaux, and D. Colson, *Phys. Rev. B* **71** B012506 (2005)
- [20] R. Nemetschek, M. Opel, C. Hoffman, P.F. Muller, R. Hackl, H. Berger, L. Forró, A. Erb, and E. Walker, *Phys. Rev. Lett.* **78**, 4837 (1997).
- [21] I. Vobornik, H. Berger, D. Pavuna, M. Onellion, G. Margaritondo, F. Rullier-Albenque, L. Forró, and M. Grioni, *Phys. Rev. Lett.* **82**, 3128 (1999).
- [22] Y. Sidis, P. Bourges, B. Hennion, L. P. Regnault, R. Villeneuve, G. Collin, and J.F. Marucco, *Phys. Rev. B* **53**, 6811 (1996); Y. Sidis, P. Bourges, H.F. Fong, B. Keimer, L.P. Regnault, J. Bossy, A. Ivanov, B. Hennion, P. Gautier-Picard, G. Collin, D.L. Milius, and I.a. Aksay, *Phys. Rev. Lett.* **84**, 5900 (2000); Y. Sidis, P. Bourges, B. Keimer, L.P. Regnault, J. Bossy, A. Ivanov, B. Hennion, P. Gautier-Picard, and G. Collin, *Cond. Mat. Phys.* **9**, 906265 (2005).